Published in final edited form as:
Nanomedicine. 2013 October ; 9(7): 912–922. doi:10.1016/j.nano.2013.02.006.

PEGylation of cationic, shell-crosslinked-knedel-like nanoparticles modulates inflammation and enhances cellular uptake in the lung

Aida Ibricevic, MD, PhD[1], **Sean P. Guntsen, BS**[1], **Ke Zhang, PhD**[2], **Ritu Shrestha, PhD**[4], **Yongjian Liu, PhD**[3], **Jing Yi Sun, BA**[1], **Michael J. Welch, PhD**[3,†], **Karen L. Wooley, PhD**[2,4], and **Steven L. Brody, MD**[1,3,*]

[1]Department of Internal Medicine, Washington University, St. Louis, MO, 63110, USA

[2]Department of Chemistry, Washington University, St. Louis, MO, 63110, USA

[3]Department of Radiology, Washington University, St. Louis, MO, 63110, USA

[4]Department of Chemistry, Texas A&M University, College Station, TX, 77843, USA

Abstract

The airway provides a direct route for administration of nanoparticles bearing therapeutic or diagnostic payloads to the lung, however optimization of nanoplatforms for intracellular delivery remains challenging. Poly(ethylene glycol) (PEG) surface modification improves systemic performance but less is known about PEGylated nanoparticles administered to the airway. To test this, we generated a library of cationic, shell crosslinked knedel-like nanoparticles (cSCKs), including PEG (1.5 kDa PEG; 2, 5, 10 molecules/polymer arm) on the outer shell. Delivery of PEGylated cSCK to the mouse airway showed significantly less inflammation in a PEG dose-dependent manner. PEGylation also enhanced the entry of cSCKs in lung alveolar epithelial cells and improved surfactant penetration. The PEGylation effect could be explained by the altered mechanism of endocytosis. While non-PEGylated cSCKs used the clathrin-dependent route for endocytosis, entry of PEGylated cSCK was clathrin-independent. Thus, nanoparticle surface modification with PEG represents an advantageous design for lung delivery.

Keywords

airway; macrophage; surfactant; alveolar epithelial cells; Poly(ethylene glycol)

Introduction

Although significant progress has been made toward developing nanoparticle (NP) carriers for drug delivery, there is an insufficient understanding regarding the optimization of

*Address correspondence to: Steven L. Brody, Washington University School of Medicine, Box 8052, 660 S. Euclid Ave, St. Louis, MO 63110, USA; Phone: (314) 362-8969; Fax (314) 362-8987, brodys@wustl.edu (for publication).
†Deceased

The authors do not have conflict of interest related to the work described in this manuscript.

particles delivered to the lung *via* the airway[1–3]. The large area of absorption of the lung represents an advantage for systemic and local delivery of NPs, and the airway offers ease of delivery. This provides the possibility that biocompatible nanocarriers may be developed for therapy and diagnosis of lung diseases[2]. However, the innate immune response and mucosal barriers are a major challenge for the effective intracellular delivery of NP in the lung[1, 4, 5]. To date, few NPs with these characteristics have been developed[6–8].

Rather than studies of therapeutic or diagnostic NP, the majority of reports related to the lung-NP interactions focus on inhalation of environmental particles (*e.g.*, carbon nanotubes, carbon black, silica, or metals) and the resulting lung inflammation or fibrosis[9, 10]. These studies also inform us that the inflammatory response is related to features that may be chemically altered to design biocompatible nanomaterials for airway delivery, including size, shape, charge, and surface characteristics[1, 10, 11].

Toward this goal, we have previously modified the size and charge of hydrogel-based NPs with a polyarginine to study the effect on lung inflammation and cell entry[12]. While some of these particles induced little significant airway inflammation, NP uptake by lung epithelial cells *in vivo* was limited[12]. To optimize NPs capable of delivery of genetic material, we have synthesized cationic, shell-crosslinked-knedel-like NPs (cSCKs). The cSCKs are derived from amphiphilic block copolymers with an acrylamide polymer-based segment that assemble as approximately 10–20 nm spheres with a hydrophobic core and highly functionalizable crosslinked shell[13–16]. Alterations in the composition and charge of the cSCK outer shell have optimized the binding capacity of payloads and transfection efficiency[16]. For example, addition of amino groups to the cSCK outer shell produces a cationic charged surface that binds plasmid cDNA or oligonucleotides through electrostatic interactions[13].

For this study, we further modified cSCKs by covalent attachment of poly(ethylene glycol) (PEG) grafts. Our rational was based on the advantages described for PEGylation of NPs that are delivered systemically, including prolonged circulation time, enhanced evasion of phagocytic cells uptake, and improved nanoparticle carriage of siRNA, DNA, proteins, and drugs[17, 18]. Also, PEGylation is reported to improve transport across a mucosal barrier and aid the movement of particles (500 nm diameter) through human mucus[19]. While particles of this size are not necessarily optimal for intracellular cargo delivery, these findings led us to hypothesize that PEGylation would enhance cSCK NP delivery in the airway. Here, we studied the effect of outer shell modifications of cSCKs with the goal to identify the most efficient, non-toxic particle that could overcome physiological barriers to target and enter alveolar epithelial cells with the ultimate goal of treatment acute and chronic lung injury[2, 20].

Methods

cSCK nanoparticles

Synthesis of cSCKs having modification of the shell with primary amines and mixtures of primary and tertiary amines were previously described[13, 16]. All solvents and chemicals were purchased from Sigma–Aldrich (St. Louis, MO). For the addition of PEG to the outer shell of cSCK, a poly(acrylamidoethylamine-*graft*-poly(ethylene glycol))-*block*-polystyrene (PAEA-*g*-PEG-*b*-PS) was generated as follows. $PAEA_{128}$-*b*-PS_{40} (20.0 mg, 1.1 μmol, 1.0 equiv.) was charged into 3 dry flasks, to which 1.7 mL DMSO was added. After stirring for 2 h, 5.5 μL (30 equiv.) of DIPEA was added to each flask. Then, 4.2 mg (2 equiv.), 10.5 mg (5 equiv.) or 21.0 mg (10 equiv.) of PEG-NHS ester (1.5 kDa) was added to each flask. Reaction mixtures were stirred overnight then transferred to pre-soaked dialysis tubing (MWCO = 12–14 kDa). Mixtures were dialyzed against 150 mM NaCl solution for 5 days,

then against nanopure water (18.0 MΩ·cm) for 2 days. After dialysis, the polymers were collected by lyophilization. Characterization of $PAEA_{128}$-g-PEG_5-b-PS_{40} is as follows.^{1}H NMR (300 MHz, DMSO-d_6): 0.80–2.42 (br, polymer backbone protons), 2.85–3.65 (br, $NHCH_2CH_2NH$, OCH_2CH_2O), 6.35–6.80 and 6.88–7.40 (br, ArH), 7.50–9.20 (br, CONH) ppm. ^{13}C NMR (75 MHz, DMSO-d_6): 31.2, 32.5–45.3 (multiple overlapping br), 70.5 (br), 125.8 (br), 127.4 (br), 128.1 (br), 145.8 (br), 175.1 (br) ppm.

Micelle formation and crosslinking procedures for the PEGylated polymers were identical to those of the non-PEGylated polymers. The cSCK particles were labeled with Alexa Fluor 488 succinimidyl ester (Life Technologies, Grand Island, NY) as previously described[15].

Characterization of nanoparticles—Physical characterization of all cSCKs, including hydrodynamic diameters (D_h), size distributions of cSCK and zeta potential (ζ) measurement were performed as previously described[16]. NPs were screened for endotoxin contamination using a Limulus Amebocyte Lysate chromogenic assay (QCL-1000, Lonza, Walkersville, MD)[21, 22]. Endotoxin levels ranged from 0.00–0.96 EU/mL.

In vivo cSCK delivery

The Animal Studies Committee of the Washington University approved these studies that were performed with humane care. C57BL/6J mice were anesthetized and sterile phosphate buffered saline (pH 7.4, PBS, Cellgro, Corning, NY) alone, or with cSCK, (30 μg/50 μL) in PBS was delivered to the trachea using a MicroSprayer (Penn Century, Wyndmoor, PA). Concentration of nanoparticles used for dosing was determined based on theoretical mass yield.

Bronchoalveolar lavage and lung tissue samples

Bronchoalveolar lavage (BAL) was performed as previously described[12]. Following BAL, lungs were inflated with 1 mL of cryopreservation media (Tissue-tek, Sakura Finetek, Torrance, CA), frozen in an ethanol bath on dry ice, then stored at −80 °C prior to sectioning. To obtain a cell suspension, lung was minced, digested in RPMI 1640 medium (Cellgro) with Liberase Blendzymes (0.28 Wunsch U/mL, Roche, Mannheim, Germany) and DNAse (5 U/mL, Sigma-Aldrich) for 90 min at 37°C. Digested lung was passed through a 70 μm cell strainer and treated with ACK Lysing Buffer (Lonza, Walkersville, MD).

Quantification of inflammatory cells and mediators in BAL

Total cells recovered by BAL were quantified and cell differential counting performed as described[12, 23]. Cell-free BAL fluid was analyzed for inflammatory mediators using the Bio-Plex Pro Mouse Cytokine 23-plex Assay (Bio-Rad, Hercules, CA) as previously described[12].

Cell culture and treatments

Cell culture—MLE 12 (ATCC, Manassas, VA), a mouse cell line with features of alveolar type II cells was cultured in media recommended by ATCC.

Pulmonary surfactant treatment—Synthetic pulmonary surfactant (Survanta, Abbott Laboratories, Columbus, OH), together with 2.5 μg of nanoparticles (final conc., 5 μg/mL) was applied to 1×10^5 cells/well. After 1 h, cells were analyzed by flow cytometry.

Endocytosis inhibitors—Inhibitors were from Sigma-Aldrich. Phagocytosis was inhibited by latrunculin B (1 μM), and macropinocytosis by cytochalasin D (10 μM) and nocodazole (33 μM). Methyl-β-cyclodextran (MβCD, 100 μM) was used to disrupt lipid raft-

mediated endocytosis by sequestration of cholesterol. Monodansylcadaverine (MDC, 200 μM) and chlorpromazine (CPM, 100 μM) were used to inhibit clathrin-mediated endocytosis, and dynasore (10 μM) to inhibit dynamin-mediated endocytosis. Cells (5×10^4/well) were pre-treated with inhibitors for 30 min, then incubated with NPs (7.5 μg/mL) for 1 h, followed by flow cytometry.

Flow cytometry

Quenching studies—cSCK labeled with Alexa Fluor 488 were co-localized in cells using a FACSCalibur flow cytometer with CELLquest software (BD Biosciences). To determine the amount of cSCK on the surface of the cell compared to that within the cell, we used rabbit anti-Alexa Fluor 488 antibody (Life Technologies) to quench the surface signal, as described[24]. Quenching efficiency was the difference between the percent cells that were Alexa Fluor 488 positive by flow cytometry prior to antibody addition, compared to post-antibody incubation.

In vivo studies—Cells obtained from BAL and lung digests were incubated with Mouse BD Fc Block (BD Biosciences) for 15 min at 4°C. BAL cells were immunostained with macrophage marker anti-mouse F4/80 (Serotec, Raleigh, NC). Lung digests were stained with hematopoietic marker anti-mouse CD45.2 (eBioscience, San Diego, CA) and pan-epithelial cell marker anti-mouse CD326 (Ep-CAM; BioLegend, San Diego, CA). Isotype control IgG antibodies were assayed in parallel. Cells were washed with PBS containing 2% fetal bovine serum, then analyzed by flow cytometry.

In vitro studies—Cells incubated with cSCKs were washed with PBS, then released from plates with Trypsin/EDTA, collected by centrifugation, washed and analyzed by flow cytometry.

Biodistribution

The PEG-cSCK and cSCK were conjugated with 1,4,7,10-tetraazacyclododecane-1,4,7,10-tetraacetic acid mono (N-hydroxysuccinimide, DOTA-NHS-ester) through the surface primary amine group for ^{64}Cu radiolabeling. In vivo biodistribution studies were performed in mice (20 to 25 g) as described[12, 25, 26]. Organs were collected, weighed, and counted in a γ-counter.

Immunostaining and microscopy

Immunostaining—Frozen tissue sections were fixed with 4% paraformaldehyde then blocked in PBS containing 0.1%Triton-X100, 3% bovine serum albumin, and 5% donkey serum as previously described[12]. Primary antibodies (and dilutions) used were: anti-prosurfactant protein C (1:1000, Abcam, Cambridge, MA), EEA1 (1:300, BD Biosciences), Lamp2 (1:100, Abcam), biotinylated anti-CD68 (1:75, Serotec), and appropriate isotype controls. Secondary antibodies included Alexa Fluor dyes (Life Technologies). Actin was stained with phalloidin Alexa Fluor 568 (1:50, Life Technologies) and nuclei with TO-PRO-3 (1:500, Life Technologies).

Colocalization of cSCK with lysosomes—Cells (5×10^4/insert) were cultured on Transwell membranes (Costar, Corning, NY) were incubated with 50 nM LysoTracker (Life Technologies) and NPs (0.5 μg/insert) for 30–120 min. Cells were fixed with 4% paraformaldehyde then stained with 4′,6′-diamidino-2-phenylindole (DAPI; Vector Laboratories, Burlingame, CA).

Colocalization of cSCK with early endosomes—Cells (1×10^4) were cultured on MatTek dishes (Ashland, MA) and labeled with early endosome marker Rab5a (Cell Light Early Endosomes-RFP BacMam 2.0, Life Technologies). After 24 h, cSCK (0.17 μg/dish) were added and cells imaged live using confocal microscopy.

Microscopy—Confocal microscopy was performed using the LSM 510 META system (Zeiss, Thornwood, NY). Epifluorescent images were captured using a Leica DM5000 microscope (Wetzlar, Germany) with a Retiga 200R camera interfaced with QCapture Pro software (Q Imaging, Surrey, BC, Canada). Photomicrographs were globally adjusted for contrast and brightness using Photoshop (Adobe Systems, San Jose, CA).

Statistical analysis

All data are represented as the mean ± standard deviation (S.D.). Groups of data were compared by the Student's t-test and one-way analysis of variance (ANOVA) with significance determined by Tukey's test with Kramer's modification. The level of significance was set at $P < 0.05$.

Results

Preparation of PEGylated cSCK nanoparticles

A series of parent cSCK particles, containing 100% primary amines (pa) (non-PEG cSCK, SCK-pa_{100}) in the shell were prepared using differing amounts of 1.5 kDa PEG grafted through amidation of portions of the primary amino groups along the block copolymer chain segment (arm) (Figure 1). The resulting cSCKs containing 2 PEG/arm were termed cSCK-2PEG (cSCK-pa_{100}-2PEG), 5 PEG/arm, cSCK-5PEG (cSCK-pa_{100}-5PEG), and 10 PEG/arm, cSCK-10PEG (cSCK-pa_{100}-10PEG). For comparison, cSCKs with the outer shell modified with differing ratios of tertiary and primary amines including: 75% primary and 25% tertiary amine (ta) (cSCK-pa_{75}-ta_{25}); 50% primary and 50% tertiary amines (cSCK-pa_{50}-ta_{50}) and 25% primary and 75% tertiary amines (cSCK-pa_{25}-t_{75})[16], were tested in parallel with the non-PEGylated parent cSCK. The mean hydrodynamic diameter and ζ-potential values of resulting cSCKs are shown (Table 1).

PEGylation of cSCK ameliorates the acute inflammatory cell response in the lung following intratracheal delivery

An acute *in vivo* screen of lung inflammation was performed following delivery of each NP. cSCKs were administered to mice intratracheally and inflammatory responses analyzed 24 h later by quantifying BAL inflammatory cells, cytokines, and chemokines. The total number of cells recovered from BAL was highest in mice that received the non-PEG cSCKs (Figure 2A). By comparison, mice receiving PEGylated cSCKs had significantly less cells (Figure 2A). Evaluation of BAL cell types following the delivery of cSCK-pa_{100}, cSCK-pa_{75}-ta_{25}, cSCK-pa_{50}-ta_{50}, cSCK-pa_{25}-ta_{75}, and cSCK-2PEG showed substantially higher numbers of neutrophils when compared to PBS (Figure 2B). The neutrophil cell response was elevated in mice that received cSCK with combinations of primary or tertiary amines, suggesting that these outer shell modifications did not differentially impact inflammation. Yet, in the 5PEG and 10PEG groups, neutrophil counts were not different from the PBS-induced response, indicating that PEGylation of cSCKs ameliorates the inflammatory response.

In agreement with the BAL cell profiles, cell-free BAL fluid from mice that received non-PEG cSCKs had increased cytokine and chemokines levels, compared to those receiving any of the PEGylated forms (Figure 2C). The significantly elevated inflammatory mediators were cytokines that function as neutrophil chemotactic factors[27]. The lowest levels of mediators were found in samples from mice receiving the highest amounts of PEG

(cSCK-10PEG). The cSCK-5PEG and -10PEG-related responses were not significantly different from PBS. Together, these data show that PEGylation of cSCKs has the capacity to reduce the inflammatory response and that this effect was directly related to amount of PEG.

PEGylation of cSCKs enhances the entry of cSCKs in lung epithelial cells

A goal of our studies was to identify a nanoparticle that was not only non-inflammatory, but could enter the cell, and was retained in the lung. Cell entry was first determined in BAL. We found a significantly higher percent of total BAL cells containing nanoparticles from mice that received cSCK-10PEG when compared to non-PEG cSCK (Figure 3A). While the total number of alveolar macrophages recovered from BAL was lower in the non-PEG than the PEG-cSCK treated mice (Figure 2B, C), the difference in percent NP uptake in alveolar macrophages (F4/80+ and CD68+ cells) was not significant (Figure 3A, right). To determine the uptake of cSCKs in the lung, we studied cell suspensions of whole lung tissue. We did not find a difference in total cell uptake of cSCKs among the mice administered different types of cSCKs (Figure 3C, left). However, analysis of the epithelial cell fraction (EP-CAM/CD326+ and CD45− cells) revealed significantly greater percent in the 5PEG and10PEG compared to non-PEG cSCKs treated mice (Figure 3C, right). Thus, PEGylation enhanced cSCK uptake in lung epithelial cells. Furthermore, biodistribution studies showed both types of radiolabeled cSCKs were highly retained in the lung, with very little extrapulmonary distribution at 24 h (Figure 3D).

PEGylation enhances the uptake of cSCKs in alveolar epithelial type II cells

The use of the EP-CAM antibody does not discriminate between the different epithelial cell types in the lung. Both non-PEGylated and PEGylated cSCK showed regional dispersal only within the alveolar compartment in lungs (Figure 4A). We did not observe cSCKs internalized within airway epithelial cells. However, both non-PEGylated and PEGylated particles could be identified within alveolar type I and type II epithelial cells. In some cases, non-PEGylated cSCK particles were associated with cell surfaces (Figure 4B) suggesting binding on the cell outer membrane, rather than entry. This was rarely observed in lung samples from mice administered cSCK-5PEG or cSCK-10PEG. Both cSCK-5PEG and cSCK-10PEG (not shown) where identified within the cytoplasm of cells with alveolar type II cell morphology (Figure 4B), and confirmed using the type II cell marker prosurfactant protein C (Figure 4C).

To better understand the enhanced entry of PEGylated particles in alveolar type II cells, we studied NP entry in the mouse MLE 12, a type II-like cell model. Similar to the *in vivo* studies, cSCK-5PEG and cSCK-10PEG demonstrated greater uptake in MLE 12 cells when compared to non-PEGylated cSCKs after 1 h (Figure 4D). To discriminate between particles binding to the cell surface and those internalized within cells, we used an anti-Alexa Fluor 488 antibody to quench fluorescent signal on the cell surface[24]. The decrease in percent cells expressing non-PEGylated cSCKs (but not PEGylated forms) after quenching (Figure 4E) suggested that a small percentage of cSCK binds to the external membrane, which may account for the presence of cSCK on the cell surface *in vivo* (Figure 4B, arrows).

We next tested the ability of PEGylated particles to penetrate pulmonary surfactant, the physiological barrier on the alveolar epithelial cell surface (Figure 4F). MLE 12 cells were treated with an artificial surfactant (Survanta) at various concentrations for 1 h. Survanta treatment decreased the relative amount of non-PEGylated and PEGylated cSCK cell entry in a concentration-dependent manner. However, Survanta markedly impaired the uptake of non-PEG cSCK compared to cSCK-10PEG. Thus, PEGylation may enhance NP internalization into alveolar epithelial cells through increased penetration through a physiological barrier.

Effect of PEGylation on intracellular trafficking of cSCKs

We also considered whether the enhanced cell uptake and internalization of 5 and 10 PEG cSCKs might be due to the differences in the endocytic pathway utilized by NPs. Both non-PEGylated and PEGylated cSCKs were localized in endosomes (marked by EEA1) and lysosomes (marked by Lamp2) in mouse lung 24 h after intratracheal NP delivery, indicating that following entry, classical pathways of trafficking were used (Figure 5A). We also observed that some NPs were intracellular but not present within endosomes or lysosomes. Given that excess free particles remained within the extracellular alveolar space *in vivo*, a dynamic process of continuous entry of NP was possible. We next asked if the difference between cell uptake of non-PEGylated and PEGylated cSCKs might be time dependent. In MLE 12 cells, we found that both PEGylated and non-PEGylated cSCKs colocalized with early endosomes at 30 min (Figure 5B) and with lysosomes after 2 hours (Figure 5C). The absence of a time-dependent difference in cell uptake led us to investigate potential differences in mechanisms of endocytosis.

PEGylation affects the mechanism for cSCK endocytosis

Accordingly, we tested the effects of well-characterized endocytosis inhibitors on non-PEG and PEG forms (Supplemental Table 1). We found no difference in uptake between the non-PEG and PEG forms when inhibitors of phagocytosis, macropinocytosis or lipid raft-mediated endocytosis were used (Supplemental Table 1). However, inhibitors of clathrin-mediated endocytosis, monodansylcadaverine (MDC) or chlorpromazine (CPM) inhibited the uptake of non-PEGylated, but not of the PEGylated cSCKs (Figure 6A).

Dynamin inhibition alone (dynasore) restricted cell uptake of both non-PEGylated and PEGylated cSCKs (Figure 6A). Dynamin inhibition was significantly greater for non-PEG than the PEG cSCKs and DECREASED directly with the extent of PEGylation. To determine the role of dynamin in the clathrin-dependent pathway, clathrin inhibitors (MDC, CPM) were tested in combination with dynasore. The combination of inhibitors did not further block entry of the non-PEG cSCKs (Figure 6B), confirming the role of dynamin in clathrin-dependent endocytosis. In sum, these results suggest that PEGylation changes the mechanisms of endocytosis, switching the cSCK uptake *via* the clathrin route, to non-clathrin pathways in alveolar epithelial cells.

Discussion

The design and delivery of NPs to the airway for therapeutic and diagnostic purposes remains a significant challenge in nanomedicine due to innate immune cell responses, airway clearance, and complex barrier functions of the lung. Although PEGylation of nanoparticles is validated for systemic delivery[17, 18], this modification has not been formally tested for lung delivery. In this study we found that PEGylation enhanced the performance of cSCK delivery to the airway by decreasing inflammatory response and improving lung epithelial cell entry, specifically in alveolar type II cells. Based on the ability to vary the number of PEG molecules on the cSCK, we found that cell entry was directly dependent on the extent of PEGylation of the cSCK outer shell. These findings suggest that PEGylation of NP is advantageous for the design of other nanomaterials as vehicles for diagnostics and therapeutics delivered to the lung, with applications for imaging and delivering genetic material[2, 20].

There are few prior reports of the beneficial impact of PEGylated NPs related to lung inflammation or lung cell uptake. Kleeman and colleagues used PEG-polyethyleneimine (PEI) coupled to TAT for the delivery of DNA by intratracheal injection[28]. While they found that TAT-PEG-PEI was an effective vehicle for DNA delivery compared to PEI

alone, both PEG and non-PEG modified forms of PEI induced high numbers of inflammatory cells recovered in BAL fluid. However, PEGylated PEI (TAT-PEG-PEI) resulted in a significantly lower neutrophil and TNF-α response when compared to PEI alone[28]. Vij and colleagues reported that intratracheal delivery of 120 nm PLGA-PEG NPs coupled to a proteasome inhibitor resulted in lower lung inflammation in a cystic fibrosis mouse model[6]. However, the specific effects of PEGylation were not studied. Similar to our finding, Hanes' group found that PEGylation of poly-L-lysine did not cause inflammation, as determined by evaluation of total immune cells in BAL at 48 hours, but there was not a direct comparison to the unmodified poly-L-lysine formulation[7].

In the lung, the precise mechanism by which PEGylation modulates inflammation is not well understood. In general, the toxicity of NPs is reported to be dependent on surface coating, charge, and particle size[10]. PEGylation can decrease the positively-charged surface that is associated with inflammation following systemic delivery of NPs[11]. It is also possible that PEGylation alters recognition of the NP by immune cells through pattern recognition receptors (pathogen-associated molecular patterns)[11, 29]. Furthermore, PEG reduces opsonization when NPs are delivered intravenously, possibly resulting in decreased macrophage activation and less inflammation[30, 31]. In our study, after intratracheal delivery the total number or percent of macrophages recovered in BAL in mice that received cSCK-5PEG or cSCK-10PEG was not different from those administered PBS (Figure 2A, 2B), indicating no increase in inflammation. However, our studies do not specifically show that PEGylation decreases uptake (i.e., opsonization) in lung monocyte/macrophage (F4/80+) (Figure 3A). In contrast to the bloodstream, the prolonged "dwell" of NP in the lung airspace may alter NP-cell contact and affect uptake. Also, we don't yet know if PEGylation will specifically decrease lung macrophage uptake, since functional phenotypes of phagocytes vary by tissue[32, 33].

We were particularly interested in the uptake of cSCK in the alveolar type II cells, as this cell type produces pulmonary surfactants, is a progenitor of the type I cell, and therefore is a candidate target for drug or gene delivery for treatment or imaging in lung injury and other lung diseases[20]. Descriptions of the efficiency of NP for delivery to lung epithelial cells *in vivo* are limited. Alveolar epithelial cells have been transfected *in vivo* using PEGylated DNA-lipid or DNA NP complexes, as determined by reporter gene expression[8, 28, 34, 35]. We found that PEGylation of NPs enhanced delivery of cSCKs into alveolar epithelial cells (Figure 4). We observed more PEGylated than non-PEG cSCK in alveolar type II cells, and fewer of both forms in type I cells. We considered that translocation of cSCK across the type I cell to the capillary network might occur. However, prior reports suggest that alveolar epithelial cell translocation of non-organic NPs is size- and charge-dependent, such that cationic NPs less than 34 nm in size are retained in the lung[3, 36]. Our biodistribution studies were consistent with this, as cSCKs (14 to 25 nm) had very low translocation from the lung (Figure 3D).

PEGylation has also been shown to facilitate the movement of NPs through physiologic mucosal barriers. We found that PEGylation enhanced cSCK penetration through a surfactant barrier *in vitro*, and may be indirectly responsible for the improved alveolar epithelial cell uptake that we observed *in vivo* (Figure 4C). Others have shown that PEGylation enhances NP movement through mucus[4, 19], however, we have not performed similar studies with PEGylated cSCK.

A major effort of our group has been to develop NPs that can bind and transfect nucleic acids[13–16]. It has been critical to first investigate the role that PEGylation of cSCKs alone have on trafficking and the mechanism of cell entry. To explain the difference in efficiency of uptake, we investigated the mechanism of cell entry using endocytosis inhibitors. While

none of the inhibitors used are absolutely specific[37], the use of multiple inhibitors and inhibitor combinations strongly suggest that PEGylation of cSCKs alters entry mechanisms. PEGylated NPs have been shown to use varied endocytosis pathways, again, related to size, charge, and shape[7, 18, 37, 38].

Positively-charged NPs may use clathrin-dependent pathways[39], though the reports concerned larger particles (80–250 nm) than we studied. Particles (less than 25 nm) are shown to use clathrin and caveolae-independent routes of entry[40]. Moreover, some particle may simultaneously utilize multiple pathways including those that are dynamin–dependent and – independent[37].

Finally, we note that these studies were performed with non-degradable particles so that the NP behaviors could be determined while they remained intact. For clinical translation, biological clearance of the nanoparticle carriers is important, as is long-term follow-up. Therefore, detailed studies that compare the behavior of non-degradable particles with degradable analogs are underway.

In conclusion, evaluation of the *in vivo* performance of a library of polymeric-based cSCK (14 to 25 nm) delivered to the lung by the airway revealed several advantages of PEG surface modification. When delivered intratracheally, PEGylation decreased the acute inflammatory response and improved NP uptake in the alveolar epithelial cells. The results were directly related to the extent of PEG on the surface and associated with an altered route of NP endocytosis. Taken together, these findings are consistent with an emerging paradigm that PEG-modification should be considered in the development of nanoparticles for payload delivery in the lung.

Supplementary Material

Refer to Web version on PubMed Central for supplementary material.

Acknowledgments

This work was supported by awards from the National Institutes of Health, including the NHLBI Program of Excellence in Nanotechnology (HHSN268201000046C) (SLB, KLW, MJW, YL) and the Children's Discovery Institute of St. Louis Children's Hospital and Washington University for the work performed by the Pulmonary Cell Culture Core (SLB). The Welch Foundation is gratefully acknowledged for partial support through the W. T. Doherty-Welch Chair in Chemistry at Texas A&M University, Grant No. A-0001 (KLW).

We thank Cassandra Mikols for performing Bio-plex assays, Adrian Shifren for assistance with statistical analysis and Mahmoud Elsabahy for helpful discussions.

Abbreviations

BAL	broncholaveolar lavage
CPM	chlorpromazine
cSCK	cationic shell crosslinked knedel-like
MβCD	methyl-β-cyclodextran
MDC	monodansylcadaverine
NP	nanoparticle
PEG	poly(ethylene glycol)
SD	standard deviation

References

1. Muhlfeld C, Rothen-Rutishauser B, Blank F, Vanhecke D, Ochs M, Gehr P. Interactions of nanoparticles with pulmonary structures and cellular responses. Am J Physiol Lung Cell Mol Physiol. 2008; 294:L817–29. [PubMed: 18263666]
2. Azarmi S, Roa WH, Lobenberg R. Targeted delivery of nanoparticles for the treatment of lung diseases. Adv Drug Deliv Rev. 2008; 60:863–75. [PubMed: 18308418]
3. Choi HS, Ashitate Y, Lee JH, Kim SH, Matsui A, Insin N, Bawendi MG, Semmler-Behnke M, Frangioni JV, Tsuda A. Rapid translocation of nanoparticles from the lung airspaces to the body. Nat Biotechnol. 2010; 28:1300–3. [PubMed: 21057497]
4. Tang BC, Dawson M, Lai SK, Wang YY, Suk JS, Yang M, Zeitlin P, Boyle MP, Fu J, Hanes J. Biodegradable polymer nanoparticles that rapidly penetrate the human mucus barrier. Proc Natl Acad Sci U S A. 2009; 106:19268–73. [PubMed: 19901335]
5. Dobrovolskaia MA, McNeil SE. Immunological properties of engineered nanomaterials. Nat Nanotechnol. 2007; 2:469–78. [PubMed: 18654343]
6. Vij N, Min T, Marasigan R, Belcher CN, Mazur S, Ding H, Yong KT, Roy I. Development of PEGylated PLGA nanoparticle for controlled and sustained drug delivery in cystic fibrosis. J Nanobiotechnology. 2010; 8:22–40. [PubMed: 20868490]
7. Boylan NJ, Kim AJ, Suk JS, Adstamongkonkul P, Simons BW, Lai SK, Cooper MJ, Hanes J. Enhancement of airway gene transfer by DNA nanoparticles using a pH-responsive block copolymer of polyethylene glycol and poly-L-lysine. Biomaterials. 2012; 33:2361–71. [PubMed: 22182747]
8. Ziady AG, Gedeon CR, Miller T, Quan W, Payne JM, Hyatt SL, Fink TL, Muhammad O, Oette S, Kowalczyk T, Pasumarthy MK, Moen RC, Cooper MJ, Davis PB. Transfection of airway epithelium by stable PEGylated poly-L-lysine DNA nanoparticles in vivo. Mol Ther. 2003; 8:936–47. [PubMed: 14664796]
9. Card JW, Zeldin DC, Bonner JC, Nestmann ER. Pulmonary applications and toxicity of engineered nanoparticles. Am J Physiol Lung Cell Mol Physiol. 2008; 295:L400–11. [PubMed: 18641236]
10. Nel A, Xia T, Madler L, Li N. Toxic potential of materials at the nanolevel. Science. 2006; 311:622–7. [PubMed: 16456071]
11. Kedmi R, Ben-Arie N, Peer D. The systemic toxicity of positively charged lipid nanoparticles and the role of Toll-like receptor 4 in immune activation. Biomaterials. 2010; 31:6867–75. [PubMed: 20541799]
12. Liu Y, Ibricevic A, Cohen JA, Cohen JL, Gunsten SP, Frechet JM, Walter MJ, Welch MJ, Brody SL. Impact of hydrogel nanoparticle size and functionalization on in vivo behavior for lung imaging and therapeutics. Mol Pharm. 2009; 6:1891–902. [PubMed: 19852512]
13. Zhang K, Fang H, Wang Z, Taylor JS, Wooley KL. Cationic shell-crosslinked knedel-like nanoparticles for highly efficient gene and oligonucleotide transfection of mammalian cells. Biomaterials. 2009; 30:968–77. [PubMed: 19038441]
14. Zhang K, Fang H, Shen G, Taylor JS, Wooley KL. Well-defined cationic shell crosslinked nanoparticles for efficient delivery of DNA or peptide nucleic acids. Proc Am Thorac Soc. 2009; 6:450–7. [PubMed: 19687218]
15. Fang H, Zhang K, Shen G, Wooley KL, Taylor JS. Cationic shell-cross-linked knedel-like (cSCK) nanoparticles for highly efficient PNA delivery. Mol Pharm. 2009; 6:615–26. [PubMed: 19231840]
16. Zhang K, Fang H, Wang Z, Li Z, Taylor JS, Wooley KL. Structure-activity relationships of cationic shell-crosslinked knedel-like nanoparticles: shell composition and transfection efficiency/cytotoxicity. Biomaterials. 2010; 31:1805–13. [PubMed: 19878990]
17. Davis ME, Zuckerman JE, Choi CH, Seligson D, Tolcher A, Alabi CA, Yen Y, Heidel JD, Ribas A. Evidence of RNAi in humans from systemically administered siRNA via targeted nanoparticles. Nature. 2010; 464:1067–70. [PubMed: 20305636]
18. Walsh M, Tangney M, O'Neill MJ, Larkin JO, Soden DM, McKenna SL, Darcy R, O'Sullivan GC, O'Driscoll CM. Evaluation of cellular uptake and gene transfer efficiency of pegylated poly-L-

lysine compacted DNA: implications for cancer gene therapy. Mol Pharm. 2006; 3:644–53. [PubMed: 17140252]

19. Lai SK, Wang YY, Hida K, Cone R, Hanes J. Nanoparticles reveal that human cervicovaginal mucus is riddled with pores larger than viruses. Proc Natl Acad Sci U S A. 2010; 107:598–603. [PubMed: 20018745]
20. Matthay MA, Zemans RL. The acute respiratory distress syndrome: pathogenesis and treatment. Annu Rev Pathol. 2011; 6:147–63. [PubMed: 20936936]
21. Neun BW, Dobrovolskaia MA. Detection and quantitative evaluation of endotoxin contamination in nanoparticle formulations by LAL-based assays. Methods Mol Biol. 2011; 697:121–30. [PubMed: 21116960]
22. Smulders S, Kaiser JP, Zuin S, Van Landuyt KL, Golanski L, Vanoirbeek J, Wick P, Hoet PH. Contamination of nanoparticles by endotoxin: evaluation of different test methods. Particle and Fibre Toxicology. 2012; 9:41. [PubMed: 23140310]
23. Gunsten S, Mikols CL, Grayson MH, Schwendener RA, Agapov E, Tidwell RM, Cannon CL, Brody SL, Walter MJ. IL-12 p80-dependent macrophage recruitment primes the host for increased survival following a lethal respiratory viral infection. Immunology. 2009; 126:500–13. [PubMed: 18783467]
24. Kozik P, Francis RW, Seaman MN, Robinson MS. A screen for endocytic motifs. Traffic. 2010; 11:843–55. [PubMed: 20214754]
25. Liu Y, Abendschein D, Woodard GE, Rossin R, McCommis K, Zheng J, Welch MJ, Woodard PK. Molecular imaging of atherosclerotic plaque with ^{64}Cu-labeled natriuretic peptide and PET. J Nucl Med. 2010; 51:85–91. [PubMed: 20008978]
26. McQuade P, Knight LC, Welch MJ. Evaluation of 64Cu- and 125I-radiolabeled bitistatin as potential agents for targeting alpha v beta 3 integrins in tumor angiogenesis. Bioconjug Chem. 2004; 15:988–96. [PubMed: 15366951]
27. Mizgerd JP. Molecular mechanisms of neutrophil recruitment elicited by bacteria in the lungs. Semin Immunol. 2002; 14:123–32. [PubMed: 11978084]
28. Kleemann E, Neu M, Jekel N, Fink L, Schmehl T, Gessler T, Seeger W, Kissel T. Nano-carriers for DNA delivery to the lung based upon a TAT-derived peptide covalently coupled to PEG-PEI. J Control Release. 2005; 109:299–316. [PubMed: 16298009]
29. Bauer RN, Diaz-Sanchez D, Jaspers I. Effects of air pollutants on innate immunity: the role of Toll-like receptors and nucleotide-binding oligomerization domain-like receptors. J Allergy Clin Immunol. 2011; 129:14–24. quiz 25–6. [PubMed: 22196521]
30. Jokerst JV, Lobovkina T, Zare RN, Gambhir SS. Nanoparticle PEGylation for imaging and therapy. Nanomedicine (Lond). 2011; 6:715–28. [PubMed: 21718180]
31. Owens DE 3rd, Peppas NA. Opsonization, biodistribution, and pharmacokinetics of polymeric nanoparticles. Int J Pharm. 2006; 307:93–102. [PubMed: 16303268]
32. Laskin DL, Weinberger B, Laskin JD. Functional heterogeneity in liver and lung macrophages. J Leukoc Biol. 2001; 70:163–70. [PubMed: 11493607]
33. Dorger M, Munzing S, Allmeling AM, Messmer K, Krombach F. Phenotypic and functional differences between rat alveolar, pleural, and peritoneal macrophages. Exp Lung Res. 2001; 27:65–76. [PubMed: 11202064]
34. Aissaoui A, Chami M, Hussein M, Miller AD. Efficient topical delivery of plasmid DNA to lung in vivo mediated by putative triggered, PEGylated pDNA nanoparticles. J Control Release. 2011; 154:275–84. [PubMed: 21699935]
35. Gautam A, Densmore CL, Golunski E, Xu B, Waldrep JC. Transgene expression in mouse airway epithelium by aerosol gene therapy with PEI-DNA complexes. Mol Ther. 2001; 3:551–6. [PubMed: 11319917]
36. Lipka J, Semmler-Behnke M, Sperling RA, Wenk A, Takenaka S, Schleh C, Kissel T, Parak WJ, Kreyling WG. Biodistribution of PEG-modified gold nanoparticles following intratracheal instillation and intravenous injection. Biomaterials. 2010; 31:6574–81. [PubMed: 20542560]
37. Luhmann T, Rimann M, Bittermann AG, Hall H. Cellular uptake and intracellular pathways of PLL-g-PEG-DNA nanoparticles. Bioconjug Chem. 2008; 19:1907–16. [PubMed: 18717536]

38. Kim AJ, Boylan NJ, Suk JS, Lai SK, Hanes J. Non-degradative intracellular trafficking of highly compacted polymeric DNA nanoparticles. J Control Release. 2012; 158:102–7. [PubMed: 22079809]

39. Dombu CY, Kroubi M, Zibouche R, Matran R, Betbeder D. Characterization of endocytosis and exocytosis of cationic nanoparticles in airway epithelium cells. Nanotechnology. 2010; 21:355102. [PubMed: 20689164]

40. Lai SK, Hida K, Man ST, Chen C, Machamer C, Schroer TA, Hanes J. Privileged delivery of polymer nanoparticles to the perinuclear region of live cells via a non-clathrin, non-degradative pathway. Biomaterials. 2007; 28:2876–84. [PubMed: 17363053]

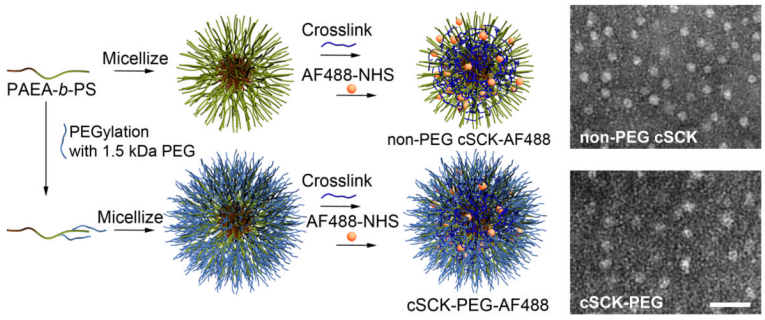

Figure 1. Synthesis and PEGylation of cationic shell-crosslinked knedel-like (cSCK) nanoparticles

The starting material was a block copolymer, consisting of a hydrophobic styrene block and a hydrophilic primary amine-bearing block (PAEA-*b*-PS). A PEG-NHS ester (1.5 kDa) was used to generate poly(acrylamidoethylamine-graft-polyethyleneglycol)-block-polystyrene (PAEA-g-PEG-*b*-PS). The process of micellization, followed by crosslinking with an activated diester of PEGylated polymers is identical to that of the non-PEGylated polymers. cSCK particles were conjugated with Alexa Fluor 488. Representative transmission electron photomicrographs show uniform size and shape of the non-PEG cSCK (parent; 100% primary amine (pa); cSCK-pa_{100}) and the particle modified with 5 of the 1.5 kDa PEG on each block-polystyrene, termed cSCK-5PEG (cSCK- pa_{100}-5PEG). Bar=50 nm.

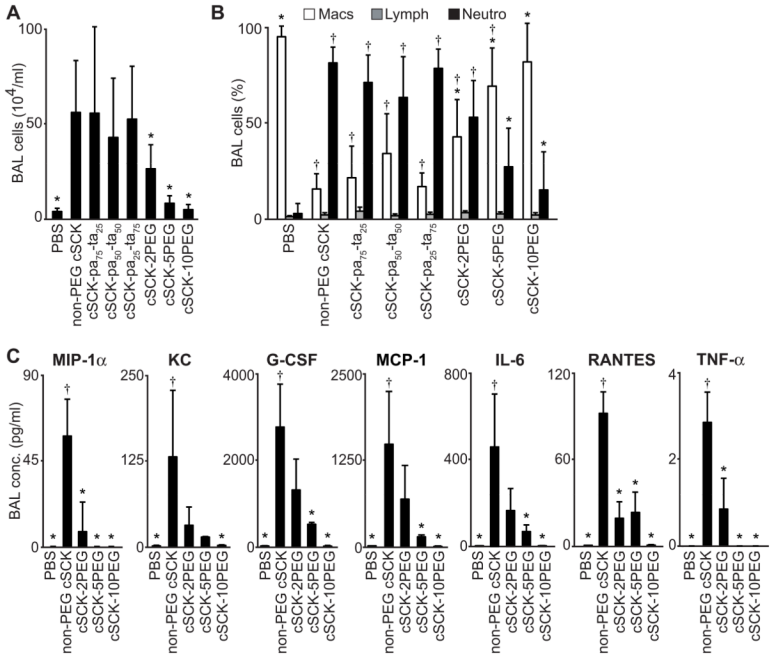

Figure 2. PEGylation of cSCK modulates the acute inflammatory response in the lung following intratracheal delivery

Mice were delivered the indicated cSCK intratracheally and evaluated by lung bronchoalveolar lavage (BAL) after 24 h. (A) Total cell number and (B) percentage of individual cell types (Mac, alveolar macrophage; Lymph, lymphocyte; Neutro, neutrophil) recovered in BAL fluid. (A, B; 9 independent experiments, n=4–6 mice/treatment) (C) Inflammatory mediators elevated in cell-free BAL fluid measured by Bio-Plex multi-analyte assay (5 independent studies, n=4–7 mice/treatment). All data are the mean ± S.D. A significant difference compared to non-PEG cSCK (*) and PBS (†) ($P < 0.05$), is indicated.

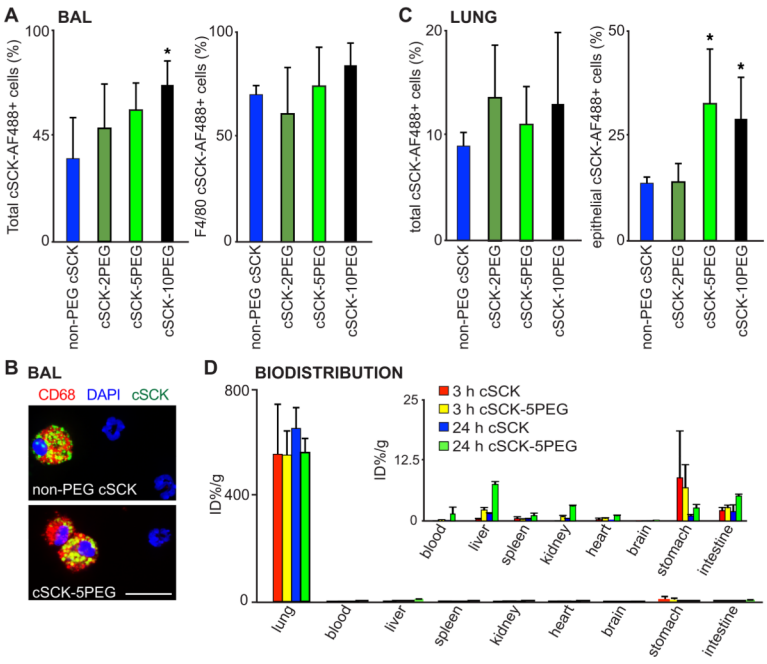

Figure 3. Uptake of cSCK nanoparticles in lung cells after intratracheal delivery of cSCK

(A) Percent of indicated cSCK labeled with Alexa Fluor 488 (cSCK-AF488) in total cells and F4/80^{+} alveolar macrophages from BAL fluid, assayed by flow cytometry. (B) Photomicrographs of cSCK within alveolar macrophages (Red, CD68^{+}) and DNA stained with DAPI (blue). Bar=20 μm. (C) Quantification of percent total (cSCK-AF488+) and lung epithelial cells (CD45−, CD326+, cSCK-AF488+) in post-BAL whole lung digests, by flow cytometry. A and C include 6 independent experiments, n=3–10 mice/treatment shown as the mean ± S.D. A significant difference compared to non-PEG cSCK is indicated (*, $P < 0.05$). (D) Biodistribution of ^{64}Cu radiolabeled cSCK in mice. Data are the mean ± S.D. percentage of injected dose (%ID) per gram of tissue (n=3–4/group at each time point). Inset shows extrapulmonary organ data.

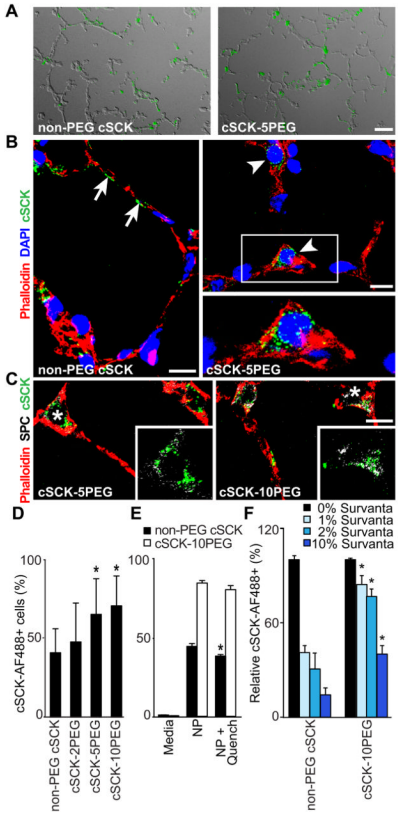

Figure 4. PEGylation of cSCKs enhances the uptake in alveolar type II epithelial cells

(A) Fluorescence photomicrographs with differential interference contrast (DIC) overlay show the distribution of fluorescent labeled cSCK in the lung alveoli. Bar=20 μm. (B, C) Confocal microscopy of cSCK in alveolar epithelial cells stained with actin marker (phalloidin, red). (B) Non-PEG cSCKs associated with the cell surface (arrows), cSCK-5PEG internalized in alveolar epithelial type II cells (arrowheads) and DNA stained with TO-PRO-3 (blue). (C) PEGylated cSCK show internalization in type II cells immunostained for prosurfactant protein C (SPC; pseudocolored white). Insets are detail of the indicated regions (*) without phalloidin stain. Bars = 10 μm in B, C. (D–F) Uptake of cSCK in MLE 12 cells detected by flow cytometry 1 h post-incubation. (D) Quantification of cSCK uptake. n=6 independent experiments with duplicate samples (E) Quenching analysis of non-PEGylated cSCK compared to PEGylated-cSCK. Cells were incubated with the indicated cSCK form, analyzed in the absence and then in the presence anti-AF488 antibody. (F) cSCK cell uptake after incubation with artificial surfactant (Survanta) relative to media only. (E, F; n=2 independent experiments with duplicate samples). All data are the mean ± S.D. A significant difference compared to non-PEG cSCK is indicated (*, $P < 0.05$).

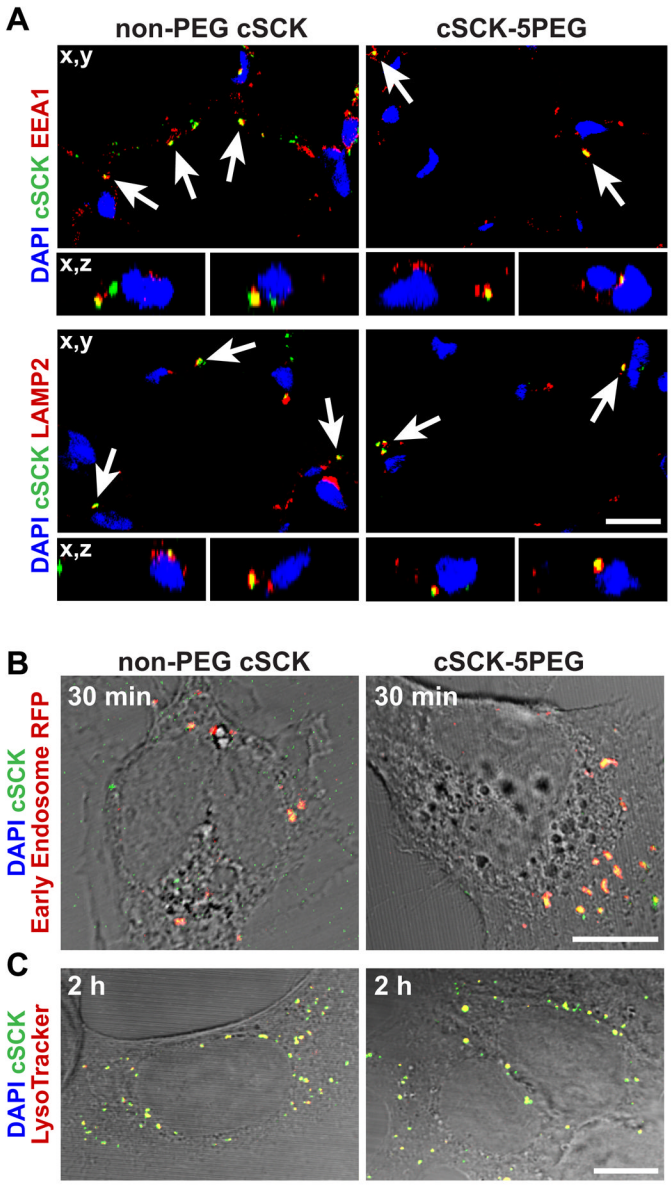

Figure 5. Intracellular trafficking of cSCK in mouse lung and MLE-12 cells

(A) Confocal image of mouse lung 24 h after intratracheal delivery of the indicated cSCK-AF488 nanoparticles immunostained with early endosomal marker protein (EEA1, red) or lysosomal marker (LAMP2, red). Colocalization is indicated (arrows). Upper panels, z-axis reconstructions; lower, x,y images (B) Top panel, cSCK-AF488 particles in MLE 12 cells, after 30 min, imaged with early endosomal marker-RFP (red) and DIC overlay. (C) Colocalization of the indicated cSCK (green) at 2 hour, with LysoTracker (red) and DIC overlay. (A, B) Bar=10 μm; (C) Bar=20 μm. Data are representative of at least 3 independent experiments.

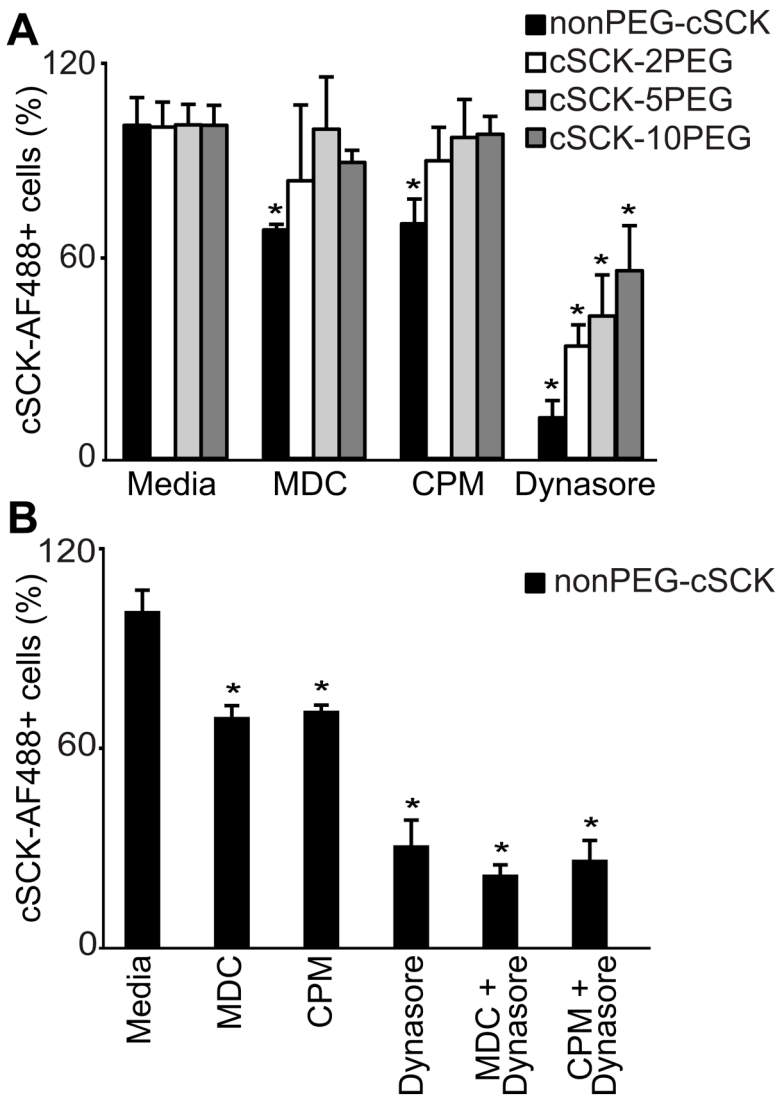

Figure 6. PEGylation of cSCK alters mechanism of endocytosis

Quantification of cSCK in MLE 12 cells by flow cytometry following pretreatment with endocytosis inhibitors. (A) Cells were pretreated with monodansylcadaverine (MDC, 200 μM), chlorpromazine (CPM, 100 μM), or dynasore (10 μM) for 30 min, then incubated with the indicated cSCK for 1 h. (B) The effect of combinations of endocytosis inhibitors on non-PEGylated cSCK uptake. Shown is the mean S.D. of six experiments with replicate samples. A significant difference in uptake compared to media is indicated (*, $P < 0.05$).

Table 1

cSCK nanoparticles and physical characteristics

Nanoparticle	Structure	ζ-potential at pH 5.5 in nanopure water (mV)	Size (nm)*
non-PEG cSCK	cSCK-pa100	21.7 ± 2.4	14 – 18
cSCK-pa75-ta25	cSCK-pa75-ta25	ND	14 – 18
cSCK-pa50-ta50	cSCK-pa50-ta50	25.0 ± 2.7	14 – 18
cSCK-pa25-ta75	cSCK-pa25-ta75	ND	14 – 18
cSCK-2PEG	cSCK-pa100-2PEG	15.4 ± 1.8	20 – 25
cSCK-5PEG	cSCK-pa100-5PEG	8.8 ± 2.5	20 – 25
cSCK-10PEG	cSCK-pa100-10PEG	1.7 ± 2.8	20 – 25

Abbreviations: pa, primary amine; ta, tertiary amine; ND, not determined

*Determined by dynamic light scatterning